J. Fluid Mech. (1972), *vol.* 54, *part* 1, *pp.* 153-161
Printed in Great Britain

On steady convection in a porous medium

By ENOK PALM, JAN ERIK WEBER
AND ODDMUND KVERNVOLD
Institute of Mathematics, University of Oslo

(Received 11 June 1971 and in revised form 31 January 1972)

For convection in a porous medium the dependence of the Nusselt number on the Rayleigh number is examined to sixth order using an expansion for the Rayleigh number proposed by Kuo (1961). The results show very good agreement with experiment. Additionally, the abrupt change which is observed in the heat transport at a supercritical Rayleigh number may be explained by a breakdown of Darcy's law.

1. Introduction

Convection in a porous medium uniformly heated from below is of considerable geophysical interest, as this phenomenon may occur within the earth. Also, the problem has an important technical application, namely to the study of the prevention of convection and thereby freezing in road and railroad constructions (frozen soil, frost heave). It is also worth mentioning that convection in porous media may provide a convenient means of experimentally demonstrating non-linear effects in convection such as the preferred cell pattern or hysteresis. In ordinary Bénard convection it is necessary to use extremely thin fluid layers to detect these phenomena (see Palm, Ellingsen & Gjevik 1967), but in porous media the friction force is much larger, so the depth of the fluid layer can be greatly increased.

The possibility of free convection in a porous medium heated uniformly from below and the similarity to Bénard convection were pointed out by Horton & Rogers (1945) and Lapwood (1948). Wooding (1957, 1958) has extended these studies, Elder (1967) and Schneider (1963) have performed laboratory experiments, and Elder (1967) has also attacked the problem by a numerical method.

In the present paper the nonlinear equations will be solved by expanding the variables using a parameter introduced by Kuo (1961) for ordinary Bénard convection. This expansion converges rapidly and gives very good agreement with observational data. The result is valid up to Rayleigh numbers about six times the critical value.

The dependence of the Nusselt number on the Rayleigh number is also found by physical arguments for moderate and high Rayleigh numbers. When the Reynolds number is increased to about one, Darcy's law ceases to be valid and new phenomena appear.

2. The equations of motion for a porous medium

The porous medium may be thought of as being composed of closely packed uniform spheres (grains) completely surrounded by a homogeneous fluid. The equations governing the motion of the porous medium for the steady case may be written as (Palm & Weber 1971)

$$-\nabla p-\rho_0\alpha T\mathbf{g}+\Sigma\mathbf{f}_s+\Sigma\mathbf{p}_s=0, \tag{2.1}$$

$$\nabla.\mathbf{v}=0, \tag{2.2}$$

$$\mathbf{v}.\nabla T=\kappa_m\nabla^2T. \tag{2.3}$$

Here p is the pressure, ρ_0 a standard density, α the coefficient of expansion, T the temperature, g the acceleration of gravity and κ_m the thermal diffusivity for the porous medium. $\Sigma\mathbf{f}_s$ and $\Sigma\mathbf{p}_s$ denote the viscous drag and pressure drag, respectively, acting on the grains within a unit volume. For small Reynolds number the total drag is a linear function of the velocity $\mathbf{v}$ (Darcy's law):

$$\Sigma\mathbf{f}_s+\Sigma\mathbf{p}_s=-(\mu/k)\,\mathbf{v}, \tag{2.4}$$

where μ is the viscosity and k the permeability.

It is assumed that the material is of infinite horizontal extent and bounded by two horizontal boundaries separated by a distance h. Also, ΔT is defined as the temperature difference between these horizontal boundaries. The field variables may then conveniently be made dimensionless by choosing

$$h,\ \Delta T,\ \mu\kappa_m/k,\ \kappa_m/h \tag{2.5}$$

as units of length, temperature, pressure and velocity respectively. Equations (2.1)–(2.3) then take the form (Wooding 1957)

$$-\nabla p+RT\mathbf{k}-\mathbf{v}=0, \tag{2.6}$$

$$\nabla.\mathbf{v}=0, \tag{2.7}$$

$$\mathbf{v}.\nabla T=\nabla^2T. \tag{2.8}$$

Here R is a Rayleigh number defined by

$$R=kg\alpha\Delta Th/\kappa_m\nu \tag{2.9}$$

and $\mathbf{k}$ is the unit vector in the vertical direction. If the horizontal boundaries are assumed to be impermeable and perfect heat conductors the critical Rayleigh number is found to be $4\pi^2$ (Lapwood 1948).

According to Schlüter, Lortz & Busse (1965) two-dimensional motion is the only stable mode for moderately supercritical Rayleigh numbers in ordinary Bénard convection. A nearly identical proof shows that this is true also for convection in a porous medium; we shall therefore consider only two-dimensional motion.

By introducing θ, defined by

$$T=T_0-z+\theta, \tag{2.10}$$

where T_0 is a standard (dimensionless) temperature, eliminating the pressure and applying the equation of continuity, we finally obtain

$$\nabla^4 w + R\nabla_1^2 w = R\nabla_1^2(\mathbf{v}.\nabla\theta), \tag{2.11}$$

$$\nabla^2\theta + w = \mathbf{v}.\nabla\theta, \tag{2.12}$$

$$\frac{\partial u}{\partial x} + \frac{\partial w}{\partial z} = 0. \tag{2.13}$$

Here the x axis is horizontal and the z axis vertical, u and w denote the horizontal and vertical velocity, respectively, and ∇_1^2 is the two-dimensional Laplacian. The boundary conditions are

$$w = \theta = 0 \quad \text{for} \quad z = 0, 1. \tag{2.14}$$

3. Solution of the nonlinear equations

Following Kuo (1960) we expand the solution in a power series in the parameter η, which is defined by

$$\eta^2 = (R - R_0)/R, \tag{3.1}$$

where R_0 is the critical Rayleigh number, so that $\eta < 1$. The solution of (2.11)–(2.13) may then be written as

$$\left.\begin{aligned} w &= \eta w^{(1)} + \eta^2 w^{(2)} + \ldots + \eta^n w^{(n)} + \ldots, \\ \theta &= \eta\theta^{(1)} + \eta^2\theta^{(2)} + \ldots + \eta^n\theta^{(n)} + \ldots. \end{aligned}\right\} \tag{3.2}$$

The Rayleigh number, which according to (3.1) is given by

$$R = R_0/(1-\eta^2), \tag{3.3}$$

may also be expanded in a power series in η or we may apply the 'finite' formula

$$R = R_0 + R_{0s}(\eta^2 + \ldots \eta^{2s}), \tag{3.4}$$

where

$$R_{0s} = R_0/(1-\eta^{2s}). \tag{3.5}$$

On expanding R_{0s} in a power series we see that R_{0s} is equal to R_0 plus terms of order higher than $2s$. Therefore, to order $2s$, R is given by (3.4) with R_{0s} replaced by R_0. However, retaining the higher order terms in R_{0s} gives just as good precision. This last procedure, which originally was proposed by Kuo (1961), leads to a more rapid convergence. With this choice of R_{0s} we are working with a correct value of R. It seems plausible that this may improve the result if the problem depends more critically on a good estimate for R than for the velocity and the temperature.

By introducing (3.2) and (3.4) into (2.11) we obtain for the first-order equation

$$\nabla^4 w^{(1)} + R_0\nabla_1^2 w^{(1)} = 0, \tag{3.6}$$

with the boundary conditions (2.14). The solution of this eigenvalue problem may be written as

$$w^{(1)} = A_1 \cos ax \sin \pi z, \tag{3.7}$$

with

$$R_0 = (\pi^2 + a^2)^2/a^2. \tag{3.8}$$

The minimum value of R_0, say R_c, is found to be

$$R_c = 4\pi^2 \quad \text{with} \quad a = \pi. \tag{3.9}$$

In the following calculations we shall assume that the horizontal wavenumber a is given by (3.9). Thus, from (2.12) and (3.7) we have, to the first order,

$$\left.\begin{aligned} w^{(1)} &= A_1 \cos \pi x \sin \pi z, \\ \theta^{(1)} &= (A_1/2\pi^2) \cos \pi x \sin \pi z, \end{aligned}\right\} \tag{3.10}$$

where the amplitude A_1 is to be determined from the nonlinear terms.

Generally the terms in (3.2) may be written as

$$\left.\begin{aligned} w^{(n)} &= A_n \cos ax \sin \pi z + \sum_{p,q} W_{pq}^{(n)} \cos pax \sin q\pi z, \\ \theta^{(n)} &= \frac{A_n}{\pi^2+a^2} \cos ax \sin \pi z + \sum_{p,q} \Theta_{pq}^{(n)} \cos pax \sin q\pi z, \end{aligned}\right\} \tag{3.11}$$

where
$$\left.\begin{aligned} W_{pq}^{(n)} &= W_{pq}^{(n)}(A_1, A_2, \ldots, A_{n-1}), \\ \Theta_{pq}^{(n)} &= \Theta_{pq}^{(n)}(A_1, A_2, \ldots, A_{n-1}) \end{aligned}\right\} \tag{3.12}$$

are nonlinear functions of the amplitudes $A_1, \ldots, A_{n-1}$. The unknown functions $W_{pq}^{(n)}$ and $\Theta_{pq}^{(n)}$ (and the amplitudes $A_1, \ldots, A_n$) are found by substituting (3.2) and (3.4) into (2.11)–(2.13) and using the fact that the coefficient of each power of η must vanish.

For the second-order terms we find

$$\left.\begin{aligned} \nabla^4 w^{(2)} + R_0 \nabla_1^2 w^{(2)} &= R_0 \nabla_1^2(\mathbf{v}^{(1)}.\nabla\theta^{(1)}), \\ \nabla^2\theta^{(2)} + w^{(2)} &= \mathbf{v}^{(1)}.\nabla\theta^{(1)}, \quad \nabla.\mathbf{v}^{(2)} = 0. \end{aligned}\right\} \tag{3.13}$$

Here
$$\mathbf{v}^{(1)}.\nabla\theta^{(1)} = \tfrac{1}{4}(A_1^2/\pi)\sin 2\pi z, \tag{3.14}$$

which gives
$$W_{pq}^{(2)} = 0, \quad \Theta_{pq}^{(2)} = \begin{cases} A_1^2/16\pi^3 & \text{for} \quad (p,q) = (0,2), \\ 0 \quad \text{for} & (p,q) \neq (0,2). \end{cases} \tag{3.15}$$

A_2 will be determined by the solvability condition for the fourth-order equation. Using (3.10) and (3.15), (2.11) gives for the third-order terms

$$\begin{aligned} \nabla^4 w^{(3)} + R_0 \nabla_1^2 w^{(3)} &= -R_{0s}\nabla_1^2 w^{(1)} + R_0 \nabla_1^2(\mathbf{v}^{(1)}.\nabla\theta^{(2)}) + R_0 \nabla_1^2(\mathbf{v}^{(2)}.\nabla\theta^{(1)}) \\ &= (\pi^2 R_{0s} A_1 - \tfrac{1}{16} R_0 A_1^3) \cos \pi x \sin \pi z + \tfrac{1}{16} R_0 A_1^3 \cos \pi x \sin 3\pi z. \end{aligned} \tag{3.16}$$

The solvability condition for this equation determines A_1, yielding

$$A_1^2 = 16\pi^2 R_{0s}/R_0. \tag{3.17}$$

Equation (3.16) then determines $W_{pq}^{(3)}$, while $\Theta_{pq}^{(3)}$ is found from (2.12).

The calculations have been carried out to sixth order, leading to

$$A_1 = 4\pi \left(\frac{R_{0s}}{R_0}\right)^{\frac{1}{2}}, \quad A_3 = 2\pi \left(\frac{R_{0s}}{R_0}\right)^{\frac{1}{2}} \left(1 + \frac{7}{24}\frac{R_{0s}}{R_0}\right),$$

$$A_5 = \frac{3\pi}{2}\left(\frac{R_{0s}}{R_0}\right)^{\frac{1}{2}} \left(1 + \frac{7}{12}\frac{R_{0s}}{R_0} - \frac{173}{3.24.24}\left(\frac{R_{0s}}{R_0}\right)^2\right),$$

$$A_2 = A_4 = A_6 = 0.$$

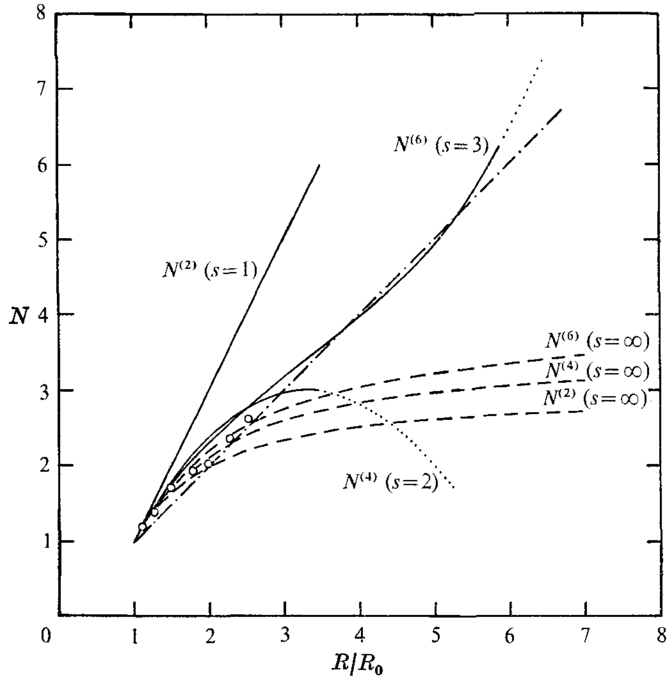

FIGURE 1. Values of N *vs.* R/R_0 for the second-, fourth- and sixth-order solutions. —·—·, general trend of various experimental data for $R/R_0 \gtrsim 2{\cdot}5$; ○, numerical values obtained by Elder (1967).

The heat transport is measured by the Nusselt number N, which is independent of z and given by

$$N = \overline{w\theta} - \partial\overline{T}/\partial z, \tag{3.18}$$

where the bar indicates a horizontal mean. Let $N^{(2)}$, $N^{(4)}$ and $N^{(6)}$ denote the second-, fourth- and sixth-order approximations, for the Nusselt number, respectively. Then, by applying our results we find

$$N^{(2)} = 1 + 2\left(\frac{R_{0s}}{R_0}\right)\eta^2, \tag{3.19}$$

$$N^{(4)} = N^{(2)} + 2\frac{R_{0s}}{R_0}\left(1 - \frac{17}{24}\frac{R_{0s}}{R_0}\right)\eta^4, \tag{3.20}$$

$$N^{(6)} = N^{(4)} + 2\frac{R_{0s}}{R_0}\left(1 - \frac{17}{12}\frac{R_{0s}}{R_0} + \frac{191}{288}\left(\frac{R_{0s}}{R_0}\right)^2\right)\eta^6. \tag{3.21}$$

4. Discussion of the solution

In figure 1, $N^{(2)}$, $N^{(4)}$ and $N^{(6)}$ are shown (solid lines) as functions of R/R_0 obtained from (3.19)–(3.21) with $s = 1$, 2, and 3 respectively. A curve illustrating the general trend of the various experimental data is also displayed in the figure. It turns out that for moderate values of R/R_0, larger than about 2·5, say, this curve is close to a straight line. Comparing our approximate results with the data,

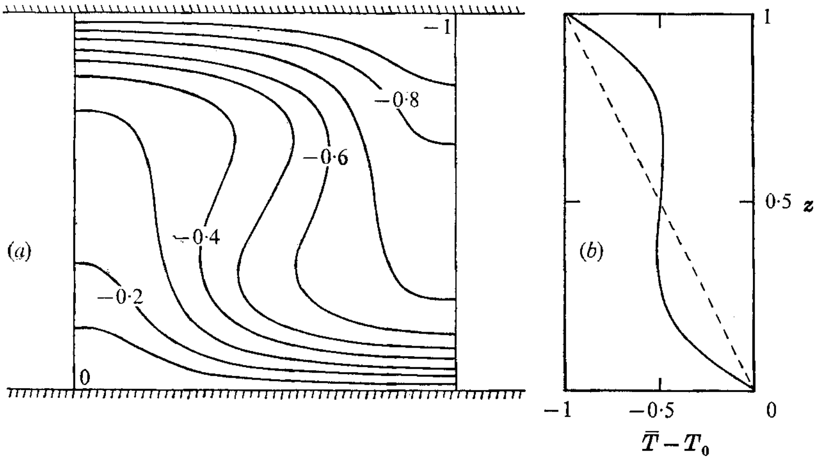

FIGURE 2. (a) Isotherms for $T-T_0$ and (b) mean temperature profile, both for $R = 3R_0$.

we see that $N^{(2)}$ is not a good approximation for any value of R/R_0, while $N^{(6)}$ is a very good approximation for $R/R_0 \lesssim 6$. For larger values of R/R_0 it obviously is necessary to take into account higher order approximations. For the sake of comparison we have also drawn the curves for $N^{(2)}$, $N^{(4)}$ and $N^{(6)}$ obtained by replacing R_{0s} with R_0 in the formulae given above. It is noteworthy that this set of values converges much less well than the first set. The values for $R/R_0 \leqslant 2{\cdot}5$ obtained by Elder (1967) using a suitable finite-difference method are also shown in this figure.

For values of R/R_0 larger than about 2·5, the isotherms and the mean temperature profile have achieved the patterns which are characteristic for moderate Rayleigh numbers (see figure 2). An approximately constant mean temperature is a typical feature of the central region, as in Bénard convection.

5. Comparison with experiments

In figure 1 the curve describing the observed data is nearly a straight line; i.e. the Nusselt number is approximately proportional to the Rayleigh number. This observed result may be made plausible by some simple physical arguments. According to (3.18) the Nusselt number may be written as

$$N = \overline{w\theta} \tag{5.1}$$

provided that the heat convection is calculated in the central region. Let us consider the heat convection through the central plane $z = \frac{1}{2}$. Assuming that at this level the friction force and the buoyancy force approximately balance each other, we have from (2.6) that

$$w = R\theta, \tag{5.2}$$

which when substituted into (5.1) gives

$$N = R\overline{\theta^2}. \tag{5.3}$$

θ is of order unity, so we may write

$$\theta \simeq \alpha \sin \pi x.$$

Since the extremal values of the total temperature $T - T_0$ occur at the horizontal boundaries, α is obviously less than $\frac{1}{2}$. From figure 2 we may estimate a value of about $\frac{1}{4}$. With this α (5.3) becomes

$$N = \tfrac{1}{32} R. \tag{5.4}$$

This is in fair agreement with the observed straight line (which is approximately given by $N = R/R_0$, where $R_0 = 4\pi$).

For larger values of R (the motion still assumed to be cellular) we may use a slightly different approach to obtain the asymptotic relationship between N and R. Now vertical as well as horizontal boundary layers will develop in the convection cell. It may be shown that the fluid outside the boundary layers (the core) is approximately isothermal. The proof is almost identical to that given by Pillow (1952) for ordinary Bénard convection. From (2.6) it then follows that the vorticity in the core is zero. Since all the streamlines are closed, the velocity in the core must also vanish. Let δ_h and δ_v denote the thickness of the horizontal and vertical layers respectively. The Nusselt number may then be written as

$$N \sim \delta_h^{-1}, \tag{5.5}$$

where $\sim$ means 'of the order of'. The formula (5.3) is still valid. It must be remembered, however, that by horizontal integration we now get contributions only from the vertical boundary layers. Equation (5.3) therefore leads to

$$N \sim R\delta_v, \tag{5.6}$$

where we have used the fact that θ is of order unity.

The last required relation is obtained by applying the heat equation in one of the vertical boundary layers. Retaining only the leading terms, we have from (2.12)

$$w\theta_z = \partial^2\theta/\partial x^2, \tag{5.7}$$

where θ_z is of order unity and w is given by (5.2). Equation (5.7) thus gives

$$R \sim \delta_v^{-2}. \tag{5.8}$$

Combining (5.5), (5.6) and (5.8), we finally obtain

$$\delta_h \sim \delta_v \tag{5.9}$$

and

$$N \sim R^{\frac{1}{2}}. \tag{5.10}$$

To our knowledge, no experimental results with which (5.10) can be compared are available.

Boundary-layer considerations in porous convection have also been applied by Elder (1967). However, he neglects the vertical boundary layers, and, instead of obtaining (5.10), finds that the Nusselt number is proportional to the Rayleigh number (as in formula (5.4)) which is true for moderate values of R.

It was mentioned above that the observed relation between R and N is nearly linear (see figure 1) for moderate Rayleigh numbers. Strictly speaking, this is only true for a porous medium composed of small grains. In the case of larger

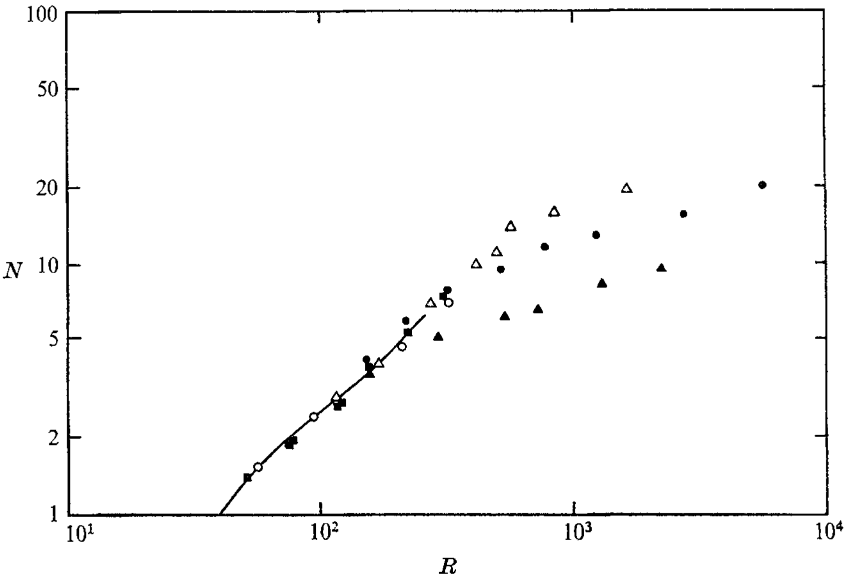

FIGURE 3. Comparison of the sixth-order Nusselt number $N^{(6)}$ with the experimental data of Schneider and Elder. ———, $N^{(6)}$, $s = 3$. Schneider (1963): ○, 4 mm glass spheres in water; ▲, 10 mm glass spheres in turpentine. Elder (1967): △, 8 mm glass spheres; ●, 18 mm glass spheres; ■, small glass spheres.

grains the observed data follow the straight line closely up to a certain Rayleigh number, the second critical Rayleigh number, whereas for still larger Rayleigh numbers the data deviate markedly from this line, as is indicated in figure 3. This deviation cannot be explained by the occurrence of horizontal and vertical boundary layers (which lead to (5.10)) since the corresponding Rayleigh numbers obviously are too small. The only explanation seems to be that at the second critical Rayleigh number Darcy's law in the form (2.4) ceases to be valid. Darcy's law in this form is valid only for Reynolds numbers less than about unity; for larger Reynolds numbers the right-hand side in (2.4) is a quadratic function of the velocity. To examine this hypothesis more closely we shall try to calculate the Reynolds numbers at which the deviations from the straight line begin. Before doing this, we mention that the phenomenon of the second critical Rayleigh number has already been studied by Schneider (1963) and Elder (1967), who both put forward the suggestion that at this point the thickness of the horizontal boundary layers have become of the same order of magnitude as the grain diameter.

A reasonable definition of the Reynolds number is

$$Re = (\overline{\langle \mathbf{v}^2 \rangle})^{\frac{1}{2}}\, d/\nu, \tag{5.11}$$

where the pointed brackets and the bar denote the mean obtained by vertical and horizontal integration, respectively. Here the velocity, the grain diameter and the kinematic viscosity are dimensional quantities. On changing to non-dimensional variables, the Reynolds number takes the form

$$Re = (\overline{\langle \mathbf{v}^2 \rangle})^{\frac{1}{2}}\, d/Pr, \tag{5.12}$$

where Pr is the Prandtl number ($= \nu/\kappa_m$). The energy equation, derived from (2.6) and (2.7), is

$$\langle\overline{\mathbf{v}^2}\rangle = R\langle\overline{w\theta}\rangle, \tag{5.13}$$

in which we have used the boundary conditions (2.14). Furthermore, from (3.18) we obtain

$$\langle\overline{w\theta}\rangle = N-1, \tag{5.14}$$

which, when combined with (5.12) and (5.13), leads to

$$Re = R^{\frac{1}{2}}(N-1)^{\frac{1}{2}}Pr^{-1}d. \tag{5.15}$$

To our knowledge, the only available observations giving the necessary information about the second critical Rayleigh number are those made by Schneider (1963), and from these we have been able to select only three different cases:

(i) Steel spheres in turpentine: $R = 60$, $N = 1{\cdot}5$, $Pr = 1{\cdot}42$, $d = \frac{15}{40}$.

(ii) Glass spheres in turpentine: $R = 180$, $N = 4$, $Pr = 4{\cdot}15$, $d = \frac{1}{4}$.

(iii) Glass spheres in water: $R = 300$, $N = 7$, $Pr = 5{\cdot}35$, $d = \frac{7}{40}$.

From (5.15) we then obtain $Re = 1{\cdot}47$, $1{\cdot}40$ and $1{\cdot}38$ for cases (i), (ii) and (iii) respectively. Thus the Reynolds numbers at which the observed data start deviating from the straight line are all very close to unity and remarkably constant. We therefore conclude that the few available experiments do support our hypothesis.

Finally, it may be worth mentioning that, by replacing Darcy's law with a quadratic velocity law, an argument similar to that leading to (5.10) gives $N \sim R^{\frac{1}{4}}$, which is in fair agreement with the observed data for Rayleigh numbers larger than the second critical value.

REFERENCES

Elder, J. W. 1967 *J. Fluid Mech.* **27**, 29.

Horton, C. W. & Rogers, F. T. 1945 *J. Appl. Phys.* **16**, 367.

Kuo, H. L. 1961 *J. Fluid Mech.* **10**, 611.

Lapwood, E. R. 1948 *Proc. Camb. Phil. Soc.* **44**, 508.

Palm, E., Ellingsen, T. & Gjevik, B. 1967 *J. Fluid Mech.* **30**, 651.

Palm, E. & Weber, J. E. 1971 *Inst. Math. University of Oslo Preprint Ser.* no. 4.

Pillow, A. F. 1952 *Aust. Dep. Supply. Aero. Res. Lab. Rep.* A 79.

Schlüter, A., Lortz, D. & Busse, F. 1965 *J. Fluid Mech.* **23**, 129.

Schneider, K. J. 1963 11*th Int. Cong. of Refrigeration, Munich Paper,* no. 11–4.

Wooding, R. A. 1957 *J. Fluid Mech.* **2**, 273.

Wooding, R. A. 1958 *J. Fluid Mech.* **3**, 582.